Bulletin of the Chemical Society of Japan

Self-Assembling and Solid-State Polymerization of Butadiyne Derivatives with Amide and Trialkoxyphenyl Groups

Kohei Kikuchi, Yoko Tatewaki, and Shuji Okada*

doi:10.1246/bcsj.20160347

Self-Assembling and Solid-State Polymerization of Butadiyne Derivatives with Amide and Trialkoxyphenyl Groups

Kohei Kikuchi,[1] Yoko Tatewaki,[2] and Shuji Okada*[3]

[1]Graduate School of Science and Engineering, Yamagata University, 4-3-16 Jonan, Yonezawa 992-8510

[2]Division of Applied Chemistry, Tokyo University of Agriculture and Technology, 2-24-16 Nakacho, Koganei 184-8588

[3]Graduate School of Organic Materials Science, Yamagata University, 4-3-16 Jonan, Yonezawa 992-8510

E-mail: kk.labmail@gmail.com

Abstract

Three butadiyne derivatives with amide and tri(dodecyloxy)phenyl (TDP) groups were synthesized, and four solidification methods were applied to obtain their self-assembling states in various conditions. The solids obtained were characterized by the solid-state polymerization behaviors, the stretching vibration wavenumbers of N-H bonds of amide groups, the powder X-ray diffraction, the thermal behaviors and the scanning electron microscope (SEM) observations. We found that all compounds had at least two polymorphs. Property differences between two polymorphs depended on the compounds. Two compounds showed clear differences in UV-Vis spectra of the photopolymerized solids, i.e., the polydiacetylene (PDA) structure and irregularly polymerized form or two PDA structures. The remaining compound showed the same PDA absorption but the monomer melting points were different. All compounds gave the gels in various organic solvents because of the molecular design with amide and TDP groups. SEM observation clarified the relationship between gel appearance and the nanostructures.

1. Introduction

Butadiyne monomers are known to be polymerized in the solid state upon UV irradiation or thermal stimuli[1] when proper monomer alignment is achieved in the self-assembling structures including the crystals. Required conditions of the butadiyne derivatives for the regular solid-state polymerization are as follows: Distance d between two monomers along the stacking direction should be about 5 Å and angle θ between the stacking direction and butadiyne moiety should be about 45° (Figure 1).[2,3] This polymerization gives stereoregular polymers and single-crystal-to-single-crystal transformation from monomers to the corresponding polymers is realized in ideal cases. It is needless to mention that this polymerization is environmentally friendly because no organic solvent is used in the polymerization process. Since the obtained polymer named polydiacetylene (PDA) has a π-conjugated polymer backbone, its functions related to optical and electronic properties have been extensively investigated.[4] Recently, PDAs have been often studied for biosensors[5] and thermosensors,[6] in which color changes by variation of effective conjugation length of PDAs were applied. Semiconducting properties of PDAs[7,8] may be applied for organic electronic devices. Donor-substituted butadiyne derivatives have been synthesized to prepare PDAs with hole transport properties[9] or to form charge-transfer complexes of PDAs.[10-12] Morphologies of PDAs have been studied not only for crystals but also for thin films,[13,14] vesicles,[15,16] gels[17] etc.

Gels of organic compounds were generally obtained by solution cooling. Recently, several gelatable butadiyne derivatives have been reported to form the corresponding PDAs.[18,19]

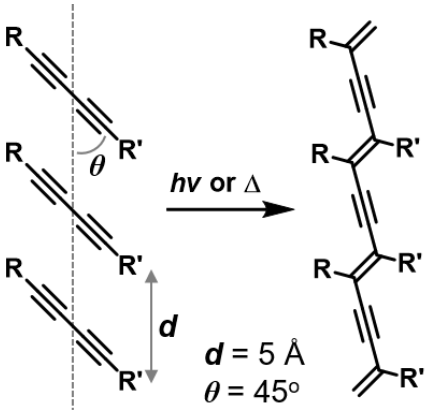

Figure 1. Solid-state polymerization of butadiyne derivatives

Most of the monomers have intermolecular hydrogen-bonding groups to promote their self-assembling in a nanometer scale. Butadiyne monomers often shows anisotropic crystal growth along molecular stacking direction, and this property results in formation of needle-like or fibrous crystals, i.e., nanofibers in a nano-environment. Such microstructures form gels in a macroscopic scale. Intermolecular hydrogen-bonding of butadiyne derivatives is also important to form the molecular packing necessary for the solid-state polymerization. Among the gelatable butadiyne derivatives so far, several types of hydrogen-bonding units such as amide[20,21] and urethane[22,23] groups were introduced. Position of the hydrogen-bonding unit in the substituents is also an important factor to determine the polymerization behaviors. Critical difference in polymerizability has been observed whether carbon number in the methylene chain between the butadiyne unit and the hydrogen-bonding group is even or odd.[24,25]

In our previous study, butadiyne derivatives with urethane and tri(dodecyloxy)phenyl (TDP) groups were synthesized as simplified gelatable compounds and their properties including polymerizability were investigated.[26] In these compounds, urethane groups were introduced to form intermolecular hydrogen-bonding and TDP groups are well known as the substituent of gelators.[27-30] Although the morphology and polymerizability of the gelatable butadiyne derivatives seem to be quite sensitive to variation, position and direction of hydrogen-bonding groups, systematic study paying attention to these factors has not been performed. In the present study, three types of inner substituents with amide group and methylene chains were introduced between the butadiyne moiety and TDP groups in the monomer. As mentioned above, amide groups were used to promote gelation and solid-state polymerization. We carried out several solidification processes for these compounds, and the macroscopic gelation ability, nanostructure morphologies, solid-state polymerizability of these compounds were investigated.

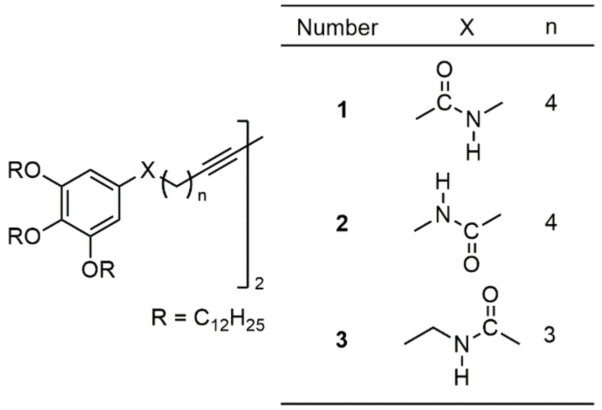

Figure 2. Structures of the butadiyne derivatives with amide and TDP groups

2. Results and Discussion

Butadiyne derivatives with TDP groups were synthesized according to Scheme 1.[31-40] The terminal hydroxylmethyl groups of **6**, **10** and **14** were transformed to aminomethyl (**9**), chlorocarbonyl (**12**) and carboxyl (**15**) groups, respectively. TDP group was prepared by dodecylation of methyl gallate **16**, and a methoxycarbonyl group of the TDP compound **17** was transformed to carboxyl (**18**), amino (**21**), and aminomethyl (**26**) groups. The acetylenic and TDP parts were combined to obtain symmetrical butadiyne derivatives with TDP groups at both ends, i.e., **1**, **2** and **3** (Figure 2). Compounds **1**, **2** and **3** are constitutional isomers each other. Direction of amide groups is opposite between **1** and **2**, and amide group position in the substituents is different between **2** and **3**. Over all yields of **1**, **2** and **3** from methyl gallate were 23%, 37% and 14%, respectively. Hereafter, compounds **1**, **2** and **3** indicate the monomers, and only their UV-irradiated samples contain the corresponding polymers.

We prepared four kinds of solids using methods (a)–(d) for each compound, i.e., (a) solvent evaporation of the chloroform solution, (b) recrystallization from chloroform-methanol mixture, (c) xerogelation using chloroform-hexane mixed solution, and (d) gelation from hexane solution of 5wt% concentration. Among them, the solids prepared by the methods (a)–(c) were obtained in the dried states. Material forms obtained by methods (a) and (b) were powders or bulk crystals. By method (c), gels were first formed and solvent evaporation of the gels afforded the corresponding xelogels. Meanwhile, by method (d), we obtained the gels, which were composed of dense fibrous structures in hexane. Solid-state polymerization of the butadiyne derivatives was first investigated by UV irradiation at 254 nm. The UV-Vis diffuse reflectance spectra, which are approximately proportional to the absorption spectra, of the samples obtained by methods (a)–(c) and the absorption spectra of the samples obtained by method (d) are shown in Figure 3. For the absorption spectra, the gels in hexane were interleaved between two quartz plates. All monomers have no absorption in visible region. Upon UV irradiation, most of the compounds showed characteristic excitonic absorption bands in visible region for the PDA backbone obtained via regular 1,4-addition polymerization (Table S1 in Supporting Information).

Among the four kinds of samples in the same compound, the spectra were the same for **3** (Figures 3 (C)). However, several differences in the same compound were observed for **1** and **2**. For **1** (Figure 3 (A)), the solids obtained by methods (c) and (d) gave the PDA structure with an excitonic absorption peak of the longest wavelength at around 570 nm. Since the solid by method (b) did not show excitonic absorption bands, regular polymerization did not progressed in this solid. For the solid by method (a), the spectrum was similar to that obtained by method (b). However, there was small absorption maximum, whose wavelength was the same as the excitonic absorption peak of the solids by methods (c) and (d). These facts suggested that there were two crystal structures, i.e., one is a regularly polymerizable form obtained by methods (c) and (d), and the other is a form obtained by method (b) with less regularity in the polymer structure. The solid by method (a) seemed to be mainly composed of the latter

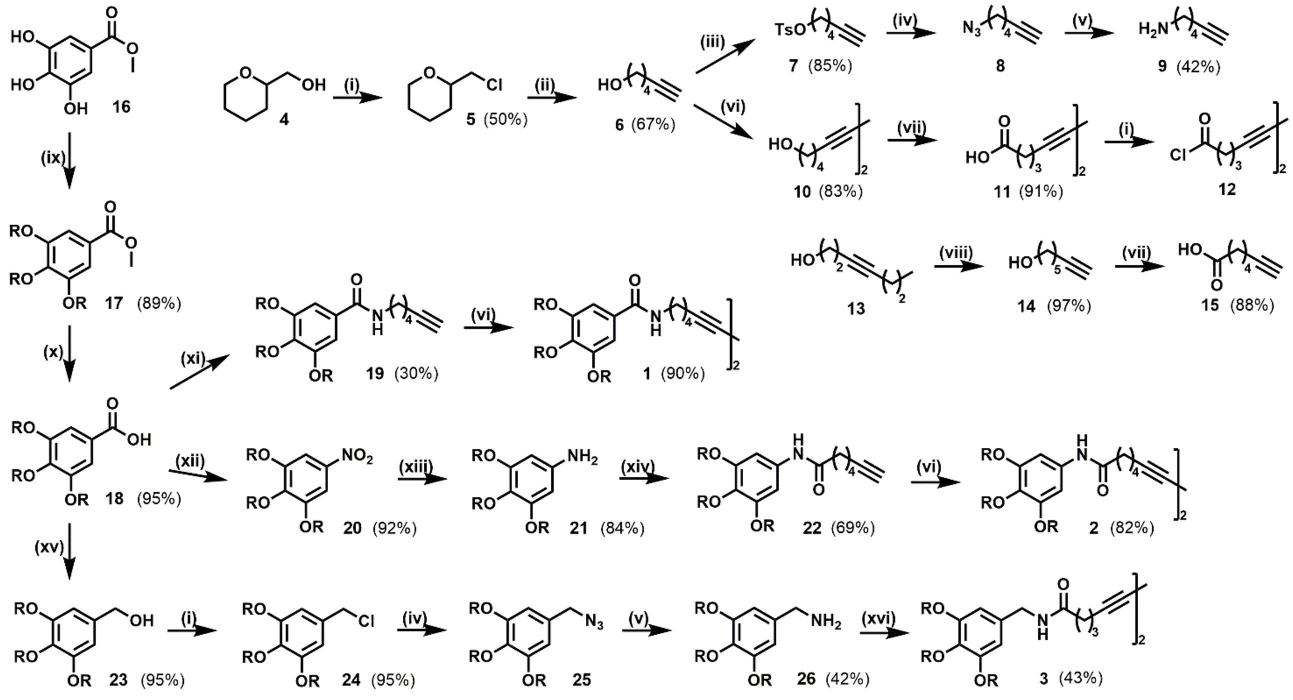

Scheme 1. Synthesis routes of **1**, **2** and **3**: (i) $SOCl_2$, pyridine, (ii) $NaNH_2$, liq. NH_3, (iii) TsCl, (iv) NaN_3, (v) PPh_3, H_2O, (vi) O_2, CuCl, TMEDA, (vii) CrO_3, H_2SO_4 aq., (viii) $H_2N(CH_2)_3NHK$, $H_2N(CH_2)_3NH_2$, (ix) $CH_3(CH_2)_{11}Br$, K_2CO_3, (x) KOH aq., (xi) **9**, DCC, (xii) HNO_3, AIBN, (xiii) $FeCl_3$, $H_2NNH_2{\bullet}H_2O$, (xiv) **15**, DCC, HOBt, (xv) LAH, (xvi) **12**, TEA. R is a dodecyl group.

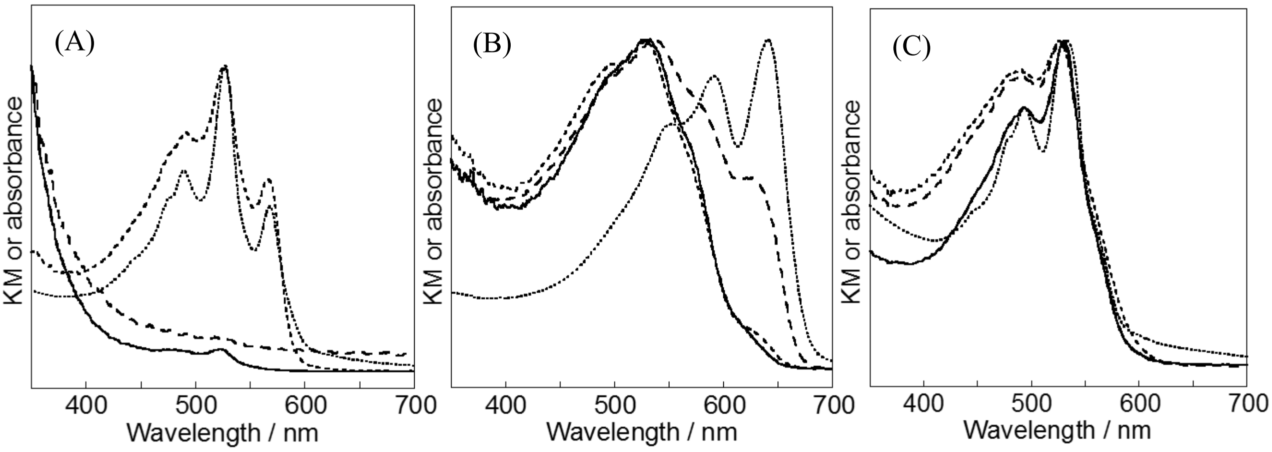

Figure 3. UV-Vis spectra of (A) **1**, (B) **2** and (C) **3** after UV irradiation. The sample preparation methods were (a) solvent evaporation of the chloroform solution, (b) recrystallization from chloroform-methanol mixture, (c) xerogelation using chloroform-hexane mixed solution, and (d) gelation from hexane solution. For the samples prepared by methods (a)–(c), the diffuse reflectance spectra were measured while absorption spectra were measured for the samples by method (d). Spectra of the solids obtained by methods (a), (b), (c) and (d) are displayed using solid, long-dashed, short-dashed and dotted lines, respectively. Each spectrum was selected from a series of spectra obtained by changing UV irradiation time so that the absorption maximum intensity became the highest. The irradiation time for each spectrum was as follows: **1** (a)–(d), 1 h; **2** (a), 1 h, **2** (b) and (c), 2 h; **2** (d), 3 min; **3** (a), 5 min; **3** (b) and (c), 30 min; **3** (d), 1 min. The spectra were normalized at the absorption maxima.

form but the former form was mixed.

In the case of **2** (Figure 3 (B)), the diffuse reflectance spectra for the solids obtained by methods (a) and (c) are the same, suggesting the same structure. The solid by method (b) also showed absorption maximum at around 530 nm. However, the absorption band extended to the longer wavelength region. The gel in hexane obtained by method (d) showed absorption maxima at 641 and 591 nm. However, after drying this sample, the absorption spectrum of the resulting xerogel shifted to shorter wavelength as shown by the dotted line in Figure 4 and it became almost the same as that of the solids obtained by methods (a) and (c). This fact suggested that the most ordered PDA structure with the longest effective conjugation length was obtained in the gel state and disorder of the PDA backbone occurred during solvent evaporation or in the recrystallization process. This consideration explains the diffuse reflectance spectrum of the solid by method (b). It mainly contained the disordered structure like the solids by methods (a) and (c) and the ordered structure like the solid by method (d) was partly remained. The spectra in Figure 3 were selected from those with the highest intensity of the absorption maximum in the course of photopolymerization. When UV was further irradiated, the maximum intensity de-

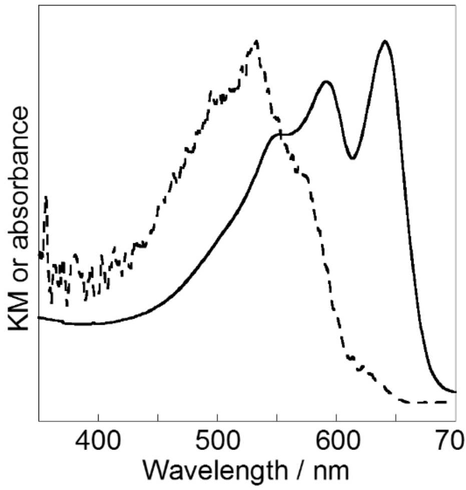

Figure 4. UV-Vis spectra of **2** after UV irradiation. Solid and dotted lines are the absorption spectrum for the gel obtained by method (d) and the diffuse reflectance spectrum of the correspoding xerogel.

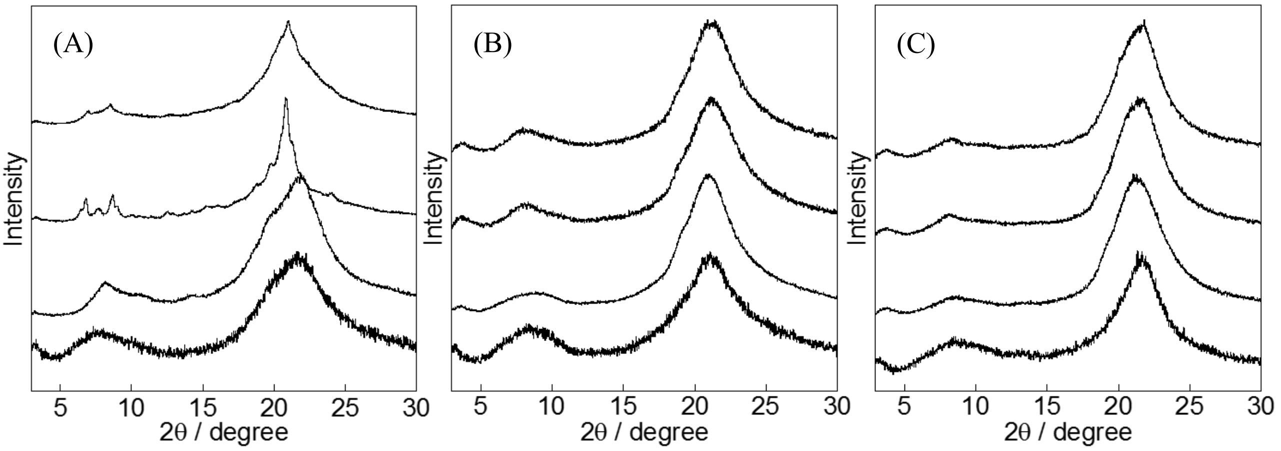

Figure 5. Poweder X-ray diffraction patterns of (A) **1**, (B) **2** and (C) **3**. Diffractograms of the solids obtained by methods (a), (b), (c) and (d) are displayed from upper to lower order. For the solids by method (d), the gel samples were dried up.

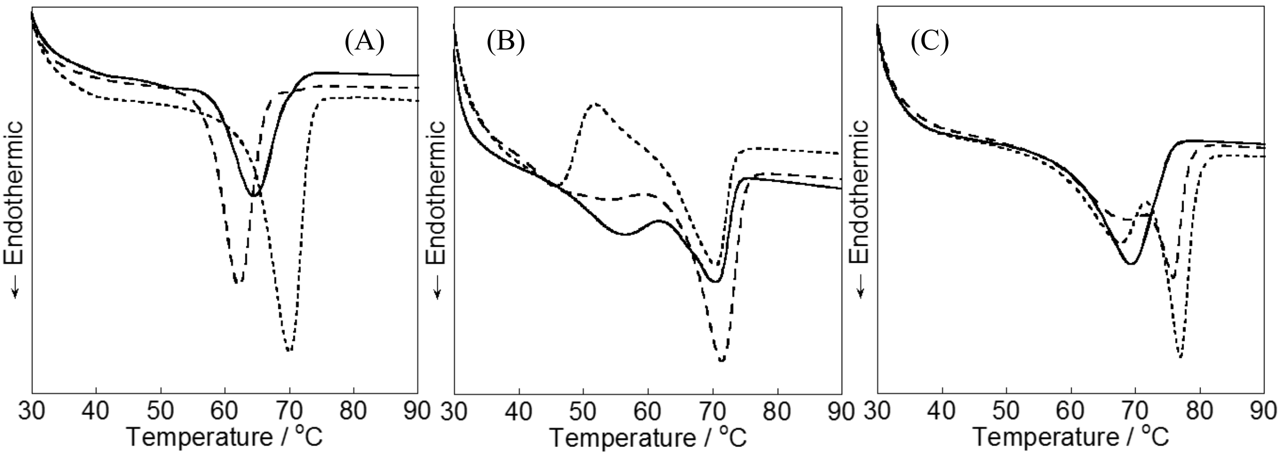

Figure 6. DSC thermograms of (A) **1**, (B) **2** and (C) **3**. Those of the solids obtained by methods (a), (b) and (c) are displayed using solid, long-dashed and short-dashed lines, respectively.

creased but the absorbance in the shorter wavelength region increased.

The powder X-ray diffraction patterns of **1**, **2** and **3** are shown in Figure 5. Broad diffraction patterns suggested that they had relatively low crystallinity. Compound **1** showed two different diffraction patterns (Figure 5 (A)), i.e., one is for the solids by method (b) and the other is for the solids by methods (c) and (d). In the diffractogram of the solid by method (a), two patterns mentioned above were overlapped. These results clearly showed existence of two polymorphs, which were consistent with the results on the UV-Vis spectra after UV irradiation. On the other hand, the diffraction patterns for **2** and **3** was generally the same among four states in the same compound (Figures 5 (B) and (C)). Although two polymorphs of **2** were unclear from the diffraction patterns, they seemed to be acceptable because the disordered states were mainly obtained after solvent evaporation of the gel states as mentioned above. All diffraction patters have a large broad peak at 2θ of around 21° and a small broad peak between 7° and 8°. The former peak corresponds to the spacing of 4.2 Å, which is related to stacking of alkyl substituents. On the other hand, the latter peak for the spacing of about 12 Å seems to be assigned as a distance between two monomers stacking arrays along the polymerization direction.

Hydrogen-bonding conditions of the solids in the dried states were compared using FT-IR spectra. Table 1 summarizes wavenumbers of stretching vibration peaks of C=O and N-H bonds. For **1**, the solids by methods (a) and (c) showed the N-H peaks at 3273±1 cm^{-1} while the solid by method (b) showed at 3266 cm^{-1}. These difference corresponds to the two polymorphs identified by the UV-Vis spectra and X-ray diffractions. For **2** and **3**, the peak position variation depending on the solidification methods was small.

Melting points and fusion enthalpies of all compounds of the solids obtained by methods (a)–(c) were evaluated by differential scanning calorimetry (DSC) (Table S2 in Supporting Information). Figure 6 shows DSC thermograms of each compound in three solid forms. All thermograms are for the first heating scans. For **1**, the solids by methods (b) and (c) corresponding to the two polymorphs showed melting points at 61.9 and 69.9 °C, respectively. The solid by method (a), which is considered to be mixture of two polymorphs, showed intermediate melting point at 64.5 °C. Compound **2** was also found to have at least two polymorphs. Although the melting points of the solids were around 71 °C, one more broad endothermic peaks were also observed between 45 °C and 60 °C and the thermal behaviors were slightly complicated. For **3**, the melting point of the solid by method (a) was 69.3 °C. However, the solids by methods (b) and (c) showed another endothermic peak at around 76 °C. These results indicated that **3** also had two polymorphs, which was not detected from the other measurements above. For all compounds, we observed the samples under a polarizing microscope with heating, and no liquid phases with birefringence were found. Although all solids of **1**, **2** and **3** showed endothermic peaks corresponding to the melting points, no exothermic peaks for crystal-

Table 1. Wavenumbers (νs) for stretching vibration of C=O and N–H of each solid state

Compound		ν /cm^{-1}		
		(a)	(b)	(c)
1	C=O	1629	1631	1631
	N–H	3272	3266	3274
2	C=O	1654	1654	1654
	N–H	3270	3272	3270
3	C=O	1643	1643	1648
	N–H	3297	3297	3295

Table 2. Gelation in various solvents[a)]

Solvent	**1**	**2**	**3**
Hexane	L (3)	L (2)	L (1)
Cyclohexane	P (3)	P (3)	P (3)
Carbon tetrachloride	–	–	–
Toluene	–	–	–
Diethyl ether	O (3)	L (2)	O (2)
Chloroform	–	–	–
Ethyl acetate	O (1)	O (2)	O (2)
THF	–	–	–
Acetone	O (1)	O (1)	O (2)
Ethanol	O (5)	O (1)	O (1)

a) Symbols in the table: P, transparent gel formation; L, translucent gel formation; O, opaque gel formation; –, no gelation even in 5wt% concentration solution. Numbers in parentheses are minimum concentration for the gel formation in wt%.

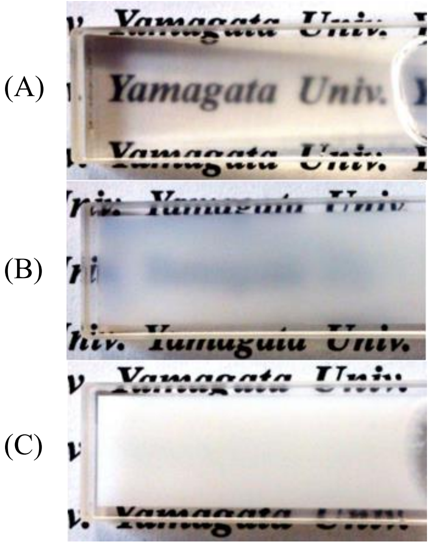

Figure 7. Appearance of (A) transparent, (B) translucent, and (C) opaque gels in cuvettes with 1-cm pass length. These gels were obtained from cyclohexane, hexane and ethyl acetate, respectively, using **1**. Classification of gel appearance in Table 2 is based on these images.

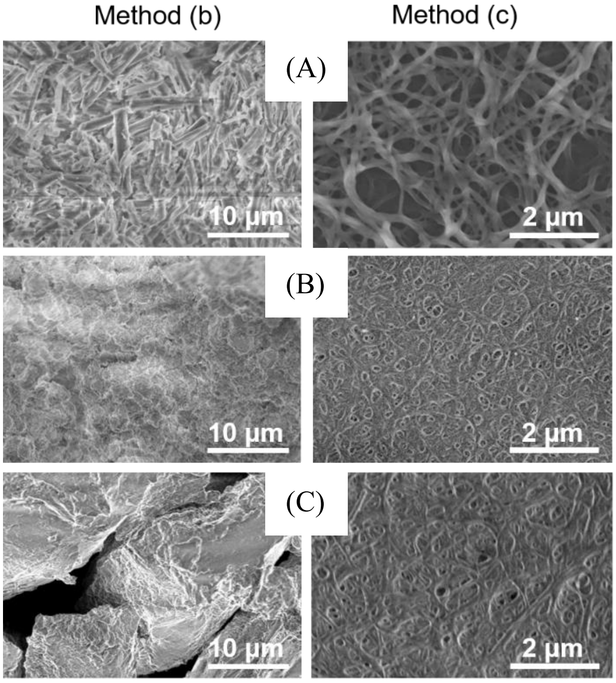

Figure 8. SEM images of (A) **1**, (B) **2** and (C) **3**. Left figures are for the solids obtained by method (b) while right figures are for the solids obtained by method (c).

lization were observed during the cooling process from the temperatures above the melting points to ambient temperature. Namely, solids obtained from the melts of these compounds were found to be amorphous.

All compounds synthesized showed gelation ability in various solvents (Table 2). Transparency of the gels varied depending on compounds and solvents, and typical appearance of the gels are shown in Figure 7. We classified the gels into three categories, i.e., transparent, translucent and opaque gels. The order of solvents from upper to lower in Table 2 corresponds to that from a small dielectric constant to large one, and it is clear that solvent dielectric constant is not simply related to the gelation ability of this series of compounds. When carbon tetrachloride, toluene, chloroform or THF was used as a solvent, the compounds were well dissolved and the gels were not obtained within 5wt% concentration of the compounds. For other combinations of the compounds and solvents, gelation was observed. As a general tendency, the non-polar solvents gave transparent gels to translucent gels, and opaque gels were formed in polar solvents. Judging from Table 2, the order of general gelation ability was estimated as follows: **1** < **2** < **3**. In **3**, the amide group is separated by a methylene group from the phenyl group, and this may cause flexibility in the conformation resulting in efficient hydrogen bonding between amide groups and π-π stacking interaction between phenyl groups to increase gelation ability.

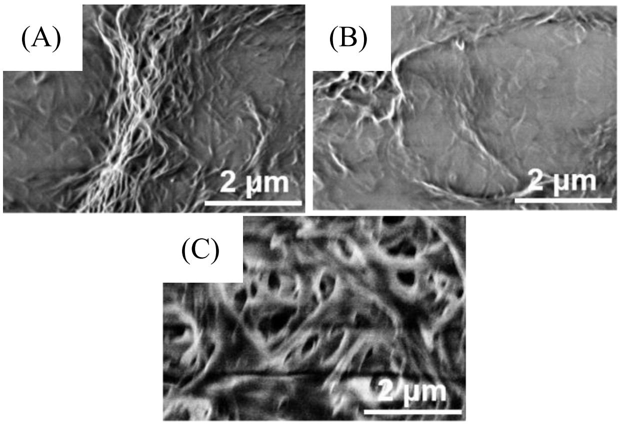

Figure 9. SEM images of **1** xerogels obtained from (A) cyclohexane, (B) hexane and (C) ethyl acetate, respectively.

Microstructures of all solids obtained were observed by scanning electron microscopy (SEM). Typical images are shown in Figure 8. In the solids obtained by method (b), bar shape structures were observed for **1** while **2** and **3** showed stacked layered structures. Minimum dimensions of these structures were more than 1 µm. Meanwhile, the xerogels obtained by method (c) generally had flexible fibrous structures, whose diameters were around 100 nm. The SEM images of xerogels of **1** obtained from three different solvents were shown in Figure 9. Figures (A), (B) and (C) correspond to transparent, translucent and opaque gels, respectively. It was found that the transparent and translucent gels were composed of fibers thinner than 100 nm. On the other hand, fibers observed in the opaque gels were thicker than 400 nm, and heterogeneous structures with sizes similar to visible light wavelengths caused scattering.

3. Conclusion

We synthesized three butadiyne derivatives with amide and TDP groups, and their self-assembling was studied by four solidification methods. The resulting solids were mainly characterized by four methods, i.e., IR spectra, powder X-ray diffraction, DSC and solid-state polymerization behaviors observed by UV-Vis spectra. Although all compounds were found to have at least two polymorphs, they were not detected by some of the four methods. From the solid-state polymerization behaviors, the polymorphisms of **1** and **2** were confirmed while those of **3** were only detected by DSC. Thus, for finding polymorphs of this type of compounds, several characterization methods must be used. Clear structural differences were observed in **1**, and the regularly polymerized form and less polymerized form were found. The longest effective π-conjugation length was obtained for the gel state of **2**, and its structure was found to disorder during the drying process. Since structural difference between **1** and **2** is only the direction of the amide groups, most of physical properties were found to be the same. However, polymerization behaviors sensitive to the arrangement of the polymerization site were altered. Compound **3** has higher gelation ability than others because of structural flexibility around the amide groups, which is responsible for intermolecular hydrogen bondings. Due to the molecular design with amide and TDP groups, all compounds gave gels in various organic solvents. From SEM observation, it was found that differences in transparency of the gels were mainly originated from differences in the nanofiber diameters. From these results, solid-state conditions of this type of compounds seems to be carefully controlled to obtain the uniform structure with desired properties.

4. Experimental

Apparatus. The UV-Vis diffuse reflectance and absorption spectra were measured using a Jasco V-570 spectrophotometer, and an integrated sphere (ILN-472) was attached to obtain the diffuse reflectance spectra. Powder X-ray diffraction patterns were measured using a Rigaku R-AXIS RAPID diffractometer with CuK_α radiation. FT-IR spectra were recorded on a Horiba FT-720 spectrometer. The melting points were measured using a SII DSC 6220 calorimeter. The nanostructures were observed using a Hitachi SU-8000 scanning electron microscope. The solid samples were put on a carbon conductive double-faced adhesive tape (Nisshin EM) mounted on an aluminum stage, and they were observed without metal coating. For identification of the compounds, NMR spectra were measured using a Jeol ECX-400 spectrometer. Elemental analysis was performed using a Perkin-Elmer CHN/O 2400 II analyzer.

Solid-state polymerization. Solid-state polymerization of the samples were stimulated using a UV lamp (UVP, UVG-11) with irradiation at 254 nm. For measurements of diffuse reflectance spectra, the solid samples were mixed and ground with KBr and the mixture were set in a holder with a quartz window, through which UV was irradiated.

Solidification methods. Four solidification methods were used. For the first one, the chloroform solutions were subjected under reduced pressure to evaporate the solvent to obtain the solids (method (a)). For the second one, the compounds were recrystallized from chloroform-methanol mixture and the solids were collected by filtration (method (b)). For the third one, the chloroform-hexane mixed solution (about 1wt%) prepared with heating were cooled to ambient temperature to form the gels, and they were filtered to obtain xerogels (method (c)). For the fourth one, the compounds were dissolved in hexane by heating to prepare the solutions with the concentration of 5wt%, and the solutions were cooled to 0 °C to form gels (method (d)). For the measurements related to Figures 4 and 5, the gel obtained by method (d) were subjected under reduced pressure and the resulting xerogels were used as samples.

Gel formation using various solvents. Twelve organic solvents were used. Ten of them are shown in Table 4. In these solvents, the compounds were dissolved in sample tubes with heating and the solutions with the concentration of 5wt% or less were prepared. Then, they were cooled in an ice bath. Definition of gel formation was that the materials inside of the tubes stayed and did not flow when the tubes were turned upside down. The remaining two solvents were methanol and acetonitrile, and they do not dissolve the compounds.

Acknowledgement

The authors thank to Mr. Rintaro Takahashi and Mr. Ryohei Tomita for their experimental works at the initial stage of this study.

Supporting Information

The absorption maximum wavelengths of the polymers, the melting points of the monomers and the synthesis procedures and the spectroscopic data of the related compounds are summarized in Supporting Information.

References

1. G. Wegner, *Z. Naturforsch.* B, **1969**, *24*, 824.
2. R. H. Baughman, *J. Polym. Sci., Polym. Phys. Ed.*, **1974**, *12*, 1511.
3. V. Enkelmann, in *Polydiacetylenes* in *Advances in Polymer Science*, ed. by H.-J. Cantow, Springer-Verlag, Berlin, **1984**, *63*, 91.
4. A. Sarkar, S. Okada, H. Matsuzawa, H. Matsuda, and H. Nakanishi, *J. Mater. Chem.*, **2000**, *10*, 819.
5. J. Deng, Z. Sheng, K. Zhou, M. Duan, C. Yu, and L. Jiang, *Bioconjugate Chem.*, **2009**, *20*, 533.
6. P. T. Hammond and M. F. Rubner, *Macromolecules*, **1997**, *30*, 5773.
7. T. Kato, M. Yasumatsu, C. Origuchi, K. Tsutsui, Y. Ueda, and C. Adachi, *Appl. Phys. Express*, **2011**, *4*, 091601-1.
8. K. Takami, J. Mizuno, M. Akai-kasaya, A. Saito, M. Aono, and Y. Kuwahara, *J. Phys. Chem. B*, **2004**, *108*, 16353.
9. M. Ikeshima, M. Mamada, H. Katagiri, T. Minami, S. Okada, and S. Tokito, *Bull. Chem. Soc. Jpn.*, **2015**, *88*, 843.
10. T. J. Savenije, J. M. Warman, H. M. Barentsen, M. van Dijk, H. Zuilhof, and E. J. R. Sudhölter, *Macromolecules*, **2000**, *33*, 60.
11. S. Ishii, S. Kaneko, Y. Tatewaki, and S. Okada, *Mol. Cryst. Liq. Cryst.*, **2013**, *580*, 64.
12. M. Imai, Y. Tatewaki, and S. Okada, *Jpn. J. Appl. Phys.*, **2014**, *53*, 05FA02-1.
13. S. Wu, F. Shi, Q. Zhang, and C. Bubeck, *Macromolecules*, **2009**, *42*, 4110.
14. D. J. Ahn, E.-H. Chae, G. S. Lee, H.-Y. Shim, T.-E. Chang, K.-D. Ahn, and J.-M. Kim, *J. Am. Chem. Soc.*, **2003**, *125*, 8976.
15. M. J. Shin and J.-D. Kim, *Langmuir*, **2016**, *32*, 882.
16. A. Potisatityuenyong, R. Rojanathanes, G. Tumcharern, and M. Sukwattanasinitt, *Langmuir*, **2008**, *24*, 4461.
17. G. N. Patel and N.-L. Yang, *J. Chem. Educ.*, **1983**, *60*, 181.
18. N. Tamaoki, S. Shimada, Y. Okada, A. Belaissaoui, G. Kruk, K. Yase, and H. Matsuda, *Langmuir*, **2000**, *16*, 7545.
19. J. M. M.-Mirabal, D. M. Aubrecht, and H. G. Craighead, *Langmuir*, **2007**, *23*, 10661.
20. G. Wang, N. Goyal, H. P. R. Mangunuru, H. Yang, S. Cheuk, and P. V. N. Reddy, *J. Org. Chem.*, **2015**, *80*, 733.
21. U. Jonas, K. Shah, S. Norvez, and D. H. Charych, *J. Am. Chem. Soc.*, **1999**, *121*, 4580.
22. J. Nagasawa, M. Kudo, S. Hayashi, and N. Tamaoki, *Langmuir*, **2004**, *20*, 7907.
23. C. Kim, S. J. Lee, I. H. Lee, K. T. Kim, H. H. Song and H.-J. Jeon, *Chem. Mater.*, **2003**, *15*, 3638.
24. H. Tachibana, R. Kumai, N. Hosaka, and Y. Tokura, *Chem. Mater.*, **2001**, *13*, 155.
25. S. Ampornpun, S. Montha, G. Tumcharern, V. Vchirawongkwin, M. Sukwattanasinitt, and S. Wacharasindhu, *Maclomolecules*, **2012**, *45*, 9038.
26. R. Takahashi, T. Nunokawa, T. Shibuya, R. Tomita, Y. Tatewaki, S. Okada, T. Kimura, S. Shimada, and H. Matsuda, *Bull. Chem. Soc. Jpn.*, **2012**, *85*, 236.
27. N. Fujita, Y. Sakamoto, M. Shirakawa, M. Ojima, A. Fujii, Ozaki, and S. Shinkai, *J. Am. Chem. Soc.*, **2007**, *129*, 4134.

28. V. Percec, J. Heck, G. Johansson, D. Tomazos, M. Kawasumi, P. Chu, and G. Ungar, *J. Macromol. Sci., Part A: Pure Appl. Chem.*, **1994**, *31*, 1719.
29. F. Würthner, S. Yao, B. Heise, and C. Tschierske, *Chem. Commun.*, **2001**, 2260.
30. J. van Herrikhuyzen, A. Syamakumari, A. P. H. J. Schenning, and E. W. Meijer, *J. Am. Chem. Soc.*, **2004**, *126*, 10021.
31. H. Gu, W. M. Xu, and T. H. Kinstle, *Tetrahedron Lett.*, **2005**, *46*, 6449.
32. Y. Yoshida, Y. Sakakura, N. Aso, S. Okada, and Y. Tanabe, *Tetrahedron*, **1999**, *55*, 2183.
33. Y. Saito, K. Matsumoto, S. S. Bag, S. Ogasawara, K. Fujimoto, K. Hanawa, and I. Saito, *Tetrahedron*, **2008**, *64*, 3578.
34. R. Takahashi, T. Nunokawa, T. Shibuya, R. Tomita, Y. Tatewaki, S. Okada, T. Kimura, S. Shimada, and H. Matsuda, *Bull. Chem. Soc. Jpn.*, **2012**, *85*, 236.
35. M. C. Sheikh, S. Takagi, T. Yoshimura, and H. Morita, *Tetrahedron*, **2010**, *66*, 7272.
36. K. K. Wang, and K. –H. Chu, *J. Org. Chem.*, **1984**, *49*, 5175.
37. E. J. Eisenbraun, *Org. Syn, Coll.*, **1973**, *5*, 310.
38. J. P. Das, P. Sinha, and S. Roy, *Org. Lett.*, **2002**, *4*, 3055.
39. V. Percec, E. Aqad, M. Peterca, J. G. Rudick, L. Lemon, J. C. Ronda, B. B. De, P. A. Heiney, and E. W. Meijer, *J. Am. Chem. Soc.*, **2006**, *128*, 16365.
40. J. Raap, S. Nieuwenhuis, A. Creemers, S. Hexspoor, U. Kragl, and J. Lugtenburg, *Eur. J. Org. Chem.*, **1999**, 2609.

Graphical Abstract

<Title>

Self-Assembling and Solid-State Polymerization of Butadiyne Derivatives with Amide and Trialkoxyphenyl Groups

<Authors' names>

Kohei Kikuchi, Yoko Tatewaki, and Shuji Okada

<Summary>

We synthesized three butadiyne derivatives with amide and tri(dodecyloxy)phenyl groups, and their self-assembling states were prepared by four solidification methods including gelation. The resulting solids were characterized by IR spectra, powder X-ray diffraction, melting points and scanning electron microscopy as well as the solid-state polymerization behaviors. Two polymorphs were found for all compounds and the good organogel formability was confirmed.

<Diagram>